

T-EMDE: Sketching-based global similarity for cross-modal retrieval

Barbara Rychalska*
Synerise
Warsaw University of Technology
Poland

Mikolaj Wieczorek*
Synerise
Warsaw University of Technology
Poland

Jacek Dabrowski
Synerise
Poland

ABSTRACT

The key challenge in cross-modal retrieval is to find similarities between objects represented with different modalities, such as image and text. However, each modality embeddings stem from non-related feature spaces, which causes the notorious 'heterogeneity gap'. Currently, many cross-modal systems try to bridge the gap with self-attention. However, self-attention has been widely criticized for its quadratic complexity, which prevents many real-life applications. In response to this, we propose T-EMDE - a neural density estimator inspired by the recently introduced Efficient Manifold Density Estimator (EMDE) from the area of recommender systems. EMDE operates on *sketches* - representations especially suitable for multimodal operations. However, EMDE is non-differentiable and ingests precomputed, static embeddings. With T-EMDE we introduce a trainable version of EMDE which allows full end-to-end training. In contrast to self-attention, the complexity of our solution is linear to the number of tokens/segments. As such, T-EMDE is a drop-in replacement for the self-attention module, with beneficial influence on both speed and metric performance in cross-modal settings. It facilitates communication between modalities, as each global text/image representation is expressed with a standardized sketch histogram which represents the same manifold structures irrespective of the underlying modality. We evaluate T-EMDE by introducing it into two recent cross-modal SOTA models and achieving new state-of-the-art results on multiple datasets and decreasing model latency by up to 20%.

1 INTRODUCTION

Cross-modal retrieval refers to expressing a single entity by means of various modalities, such as image, text or sound. For example, a garden party scene can be identified either by its photo, textual description ("*a group of people laughing and talking*"), or the recorded sound of the scene. Image-text matching is particularly common, e.g. in database retrieval tasks of photos via their textual descriptions [14, 18, 33], image captioning [22, 24, 57], and multimodal neural machine translation [25, 36].

Cross-modal matching remains a challenge due to the 'heterogeneity gap', caused by the fact that modalities are represented by inherently nonmatching feature spaces [15, 32, 50]. Cross-modal methods strive to bridge the gap with various neural architectures, such as Graph Neural Networks (GNNs) and multiple forms of attention [6, 15, 31, 51, 60] in order to compute per-modality vectors which can be compared. The similarity (or distance) between these vectors is used to compute the probability of a correct match between image and caption. Unfortunately, both GNNs and attention

networks are known for poor scalability and specific performance issues [3, 7, 59].

An important flavor of attention which is often found in cross-modal systems is the self-attention. It is used in various deep learning domains to obtain a summary representation of text or image. Self-attention has proven very successful, especially in the Transformer architecture [46], which has led to many performance breakthroughs in areas such as machine translation, language modeling, and image classification [16, 38, 42, 53]. Yet, the core operation of self-attention is the dot product between a sequence representation and itself, which results in quadratic complexity. This characteristic makes self-attention inefficient in many real-life industrial applications. For this reason, attempts are made at devising more efficient architectures which could replace self-attention [4, 47].

In this paper we address the above mentioned problems with an efficient neural module which can serve as a drop-in replacement for self-attention, which we call T-EMDE. Our proposed solution is especially appropriate for computation of global representations of text and image in multimodal retrieval scenarios. T-EMDE is inspired by the recently introduced EMDE (Efficient Manifold Density Estimator) [17] which has proven competitive in multimodal recommendation scenarios. We design T-EMDE with three main goals in mind:

- **High efficiency.** T-EMDE has linear complexity with respect to the sequence size (text tokens or image segments). This stands in contrast to quadratic complexity of self-attention.
- **Unified cross-modal representation.** T-EMDE maps any modality to the same type of representation - a semi-histogram on multidimensional data manifolds. This unified representation bridges the problem of heterogeneity gap.
- **Differentiability.** While the EMDE architecture has been shown to achieve high results and avoid scalability problems characteristic for complex neural architectures, it is a non-differentiable algorithm which prevents the fine-tuning of embeddings. With T-EMDE we exploit the same ideas which give EMDE its advantages, while making it fully trainable.

We evaluate T-EMDE by introducing it into two recent high-performing models which use self-attention: SAF (Similarity Attention Filtration) and SGR (Similarity Graph Reasoning) [15]. By introducing T-EMDE, we are able to reach new state-of-the-art results on MSCOCO and Flickr30k datasets. We observe especially significant gains in the Recall@1 metric, representing the quality of the top returned recommendation. In multiple cases, the gains in Recall@1 are well over 1 pp. with comparison to the baseline SAF and SGR. At the same time, due to reduced complexity T-EMDE lowers model inference latency by up to 20%. We propose T-EMDE

*Both authors contributed equally to this research.

as a step in the direction of replacing computationally expensive self-attention with more efficient approaches.

2 RELATED WORK

2.1 Text-image alignment

A number of prior works [19, 48, 62] focused on matching global image and text features in a joint embedding space. The aim was to learn to map both modalities to the same vector space, where the similarity measure could be applied for the cross-modal retrieval. One of the shortcomings of methods using only global representation was their ignorance of the fact that the notion of similarity may arise from an aggregation of numerous local similarities, such that salient objects in the image and keywords in the text. To address the problem, [26] explored mutual relations between image regions and words in text. The authors proposed to infer a similarity score between each pair of an image region and each word to define the alignment of the corresponding fragment features in the shared embedding space. This approach of computing similarity on the level of a smaller units from each modality was explored in many subsequent works.

Since the Transformer architecture proved successful in various domain, the self-attention mechanism has been explored by many researchers in cross-modal retrieval settings [6, 15, 23, 31, 41, 52, 60]. [51] introduced Position Focused Attention Network (PFAN), which incorporates object position clues into the learning architecture. Images are split into blocks and attention mechanism is used to generate meaningful region features that are later fed into visual-textual attention to learn the joint-embedding space. [8] proposed Dual Path Recurrent Neural Network (DP-RNN), which symmetrically processes images and sentences. It ‘reads’ the image objects in the order the text indicates, reorders them based on the object-word matching and an RNN learns joint information embeddings of semantically related objects. Finally, a module consisting of attention and self-attention mechanism is applied to compute the image-text similarity from recurrent visual and textual features. [60] observe that many attention-based methods ignore the fact that image segments or words might have various semantic meaning that depends on the global context, which in turn was defined as intra-modal and inter-modal relations. They devised Context-Aware Attention Network (CAAN), which aggregates context information of alignments between modalities and within a single modality simultaneously. [6] proposed to use Iterative Matching with Recurrent Attention Memory (IMRAM) method to capture the mutual image and text alignments iteratively. It consists of two main parts: (1) a cross-modal attention applied multiple times that builds the fine-grained correspondence between modalities progressively, (2) a memory distillation unit which aggregates alignment knowledge from earlier steps and passes it to later ones.

[32] is an example of a Graph Convolutional Network model which generates visual features of salient objects and their semantic relationship. The gate and memory mechanism [12] is used to perform semantic reasoning, which considers both local and global semantic correlations. It enables the model to select information that contributes to a meaningful representation of the whole scene and ignore redundant cues at the same time. [50] introduces Scene Graph Matching (SGM) - an approach using separate graphs for

each modality to capture object features and their mutual relationships in corresponding modality. When the object-level and relationship-level features are extracted from both modalities, the final matching on both levels takes place.

[31] proposed Stacked Cross Attention Network (SCAN), which is trained to discover the full latent alignment between salient objects and words. The SCAN can be defined as two complimentary formulations, where each modality is used as a context to each other and two separate similarity scores are inferred. The alignment is done on the local-region level, which is next aggregated to build a global representation. While SCAN used the cross-modal attention with success it lacked the self-attention part. [15] builds upon SCAN, extends it with self-attention and applies it to each modality separately. It introduced two modules - Similarity Attention Filtration (SAF) and Similarity Graph Reasoning (SGR) to boost the accuracy of alignments between modalities. SGR is based on a graph convolutional neural network (GCNN). It builds a similarity graph that propagates similarities at local and global levels to obtain the alignment scores. Similarity Attention Filtration (SAF) module was introduced as the authors noticed that using the local alignments generally boosts the performance, but incorporating the less relevant elements into the global representation decreases the final results. SAF aim is to decide which alignments are significant and which should be filtered out. The SGRAF model is an ensemble of SRG and SAF models, which similarity scores are averaged before the retrieval takes place.

2.2 Attention Mechanism

Attention is a mechanism that allows the network to learn correspondence between input and target sequence/set elements. One of the first works that introduced the popular attention mechanism was [2]. The authors proposed a simple additive module that computed ‘attention scores’ for each input element. The weights of the alignments were computed by feeding RNN hidden state and a word latent vector into a single-layer feedforward neural network. This allowed the RNN decoder to attend to any part of the source sentence and in turn it increased the quality of machine translation task. A similar approach can be found in Computer Vision, where attention was used to help the network find relevant images patches and object in the image to generate captions [55].

The Transformer architecture [46] introduced a scaled dot product self-attention computed over three elements: the Query, Key, and Value. This can be deemed as an extension of the attention from [2]. The Transformer architecture computes the self-attention multiple times separately, which is known as multi-head attention. According to the authors this allows the model to attend to information from different representation subspaces at different positions. Furthermore, the attention mechanism was extended by residual connections and normalization layers. Transformer model and its self-attention mechanism has started to dominate various domains. For example, it achieved state-of-the-art results in machine translation [38, 45], text summarizing [38], visual question answering [42, 43].

However, the Transformer architecture is notorious for its difficulty to train and its demand for large amounts of data. Most

current state-of-the-art solutions in cross-modal retrieval are non-Transformer models, which nevertheless use simplified dot-product self-attention modules commonly [6, 15, 23, 31, 41, 51, 56, 56, 61].

2.3 Optimizing Self-Attention

Unfortunately, the time and memory complexity of self-attention is quadratic as it needs to compute the weights between each pair of inputs. It prevents efficient scalability of attention-based models, especially where longer sequences are present in the data. To tackle this problem many researchers introduced the extensions and improvements, which are however primarily dedicated for the Transformer architecture.

Some works attempt to limit Transformer self-attention by attending only to some inputs according to a fixed block/patterns [5, 9, 13, 37, 44]. Another approach to improve the complexity of Transformer self-attention is to use low-rank factorization methods. [45, 49] assumed low-rank structure of self-attention. They project the Transformer Key and Value vectors into a lower-dimensional representation. Some works [11, 27] used kernel functions to bring down the dimensionality of the elements on which the Transformer self-attention operates. [40, 54] introduced centroids/clusters into the Transformer self-attention. The idea is to calculate the attention scores only among the tokens belonging to the same cluster/centroid. [28] proposed Transformer LSH Attention, which uses Locally-Sensitive Hashing method to obtain hashes for both the Keys and the Queries.

Thus, most attempts at limiting the complexity of self-attention are dedicated for the Transformer’s formulation of self-attention, assuming the creation of multiple Query, Key, Value vectors to build multi-head attention within a strictly defined neural architecture. Yet, few attempts are made at optimization or replacement of the basic formulation of (self) attention. This comes at a disadvantage to models in which the simple classic attention composed of a single dot product and weighted summation of vectors is the preferred choice [15, 23, 51, 56]. With T-EMDE, we mean to bridge the gap by introducing a conceptually simple and fast alternative to classic self-attention. Additionally, we aim at easy communication between various modality representations, which is not handled inherently by neither formulation of attention.

3 PROPOSED METHOD

In this section we describe the following architectures: EMDE [17] which serves as an inspiration model, T-EMDE - our proposed module, and SAF/SGR [15] - models which serve as scaffolds into which T-EMDE is introduced.

3.1 Non-Trainable Efficient Manifold Density Estimator

Efficient Manifold Density Estimator (EMDE) introduced in [17] is a probability density estimator inspired by Count-Min Sketch algorithm (CMS) and local sensitive hashing (LSH). The overview of the algorithm is shown in Figure 2. EMDE ingests input data represented by vectors embedded on manifolds spanned by various upstream representation learning methods. The manifolds are then partitioned via a data-dependent LSH method (DLSH). The partitioning method divides the manifold into regions, analogous

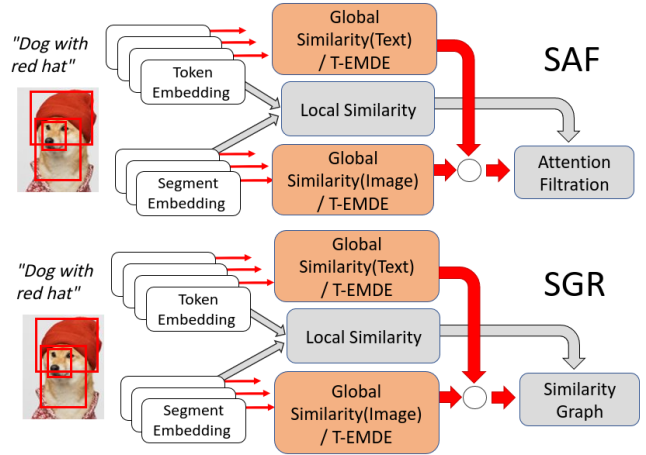


Figure 1: An overview of the SAF and SGR architectures, showing where T-EMDE is introduced.

to CMS buckets. The purpose of manifold partitioning follows the logic of LSH: similar data points should be mapped to the same region. While a single region is large (typically 64-256 regions form a single partitioning covering the whole manifold, as described in [17]), multiple independent partitionings allow to obtain a high resolution map of the manifold via intersection or ensembling.

The resulting region assignment vectors (*sketches*) can be thought of as a form of a histogram. Each position within a sketch corresponds to a region, and each value represents the number of data points in the given region. For example, a sketch of a single item can take the form of $I = [0, 0, 1, 0, 0]$, which means that the data point in question is located in region number 2 out of 5 total regions. All items are represented with sketches of the same dimensionality, and representations of item sets are computed by simple summation of individual item sketches. For example, a shopping basket of 4 items can be represented with as sketch $S = [1, 0, 2, 0, 1]$ containing 4 items in total, one located in region number 0, two in region number 2, and one in region number 4. EMDE precomputes sketch representations of all items within the inventory, computes aggregate shopping basket sketches, and uses simple feed-forward network for mapping a basket sketch to a predicted sketch of items which will be likely bought next.

The algorithm is shown to achieve competitive results in product recommendation settings, which are often multimodal. Products can be characterized by user interactions (e.g. assignment to shopping baskets), textual descriptions, photos, and categorical features. In EMDE, all per-modality representations are transformed to the histogram-like sketches, which follow the same logic irrespective of the underlying modality or representation method. EMDE is shown to be fast and efficient - thanks to the application of the hashing-based CMS structure, it works in sublinear space. The neural architecture of EMDE is very simple, with just feed-forward layers.

However, in [17] the DLSH method is neither differentiable nor end-to-end trainable, due to the highly discontinuous binary-unary conversion being a key operation during assignment of inputs to

region indices. Thus, manifold partitionings must be precomputed before actual training and are based on pretrained vectors, which prevents the model from learning own embedding vectors or fine-tuning embeddings derived from upstream representations. A drop-in replacement module for attention must be trainable, as otherwise it would block off the gradient in a whole portion of the underlying network. In particular, cross-modal architectures often do not use precomputed embeddings but rather train their own representations from scratch, which makes it obligatory for all parts of the network to be differentiable.

3.2 Trainable Efficient Manifold Density Estimator

Taking into the account all key characteristics which an attention replacement module should possess, we introduce the T-EMDE as a trainable version of EMDE. We retain the core properties of EMDE: high scalability due to the application of a hashing-based data structure and a unified representation used for all modalities to bridge the heterogeneity gap. Moreover, we aim to retain the ability of EMDE to model item sets, which in our case will be sets of tokens and image segments. The ability of computing a single object representation out of its composing part sequence (of variable size) makes T-EMDE a valid candidate for replacing self-attention.

T-EMDE aims to partition the underlying data manifold, similarly as EMDE. However, instead of a static assignment of inputs to specific regions of the manifold, we propose to use trainable centroids. The centroids are created within a space of arbitrary dimensionality and represent the basis of item representation - each token/image segment will be characterized by a vector of distances to all centroids. An overview of EMDE is shown in Figure 1, presenting its application to multiple modalities.

Our algorithm proceeds as follows:

- 1. Centroid initialization.** We initialize a trainable centroid tensor C of dimensionality $N \times K \times D$. The tensor will hold K centroids for each of N independent manifold divisions. Independent manifold divisions are introduced with regard to the observation from [17] that a single manifold partitioning will usually not be perfect and multiple independent divisions can achieve an ensembling effect, which is beneficial to performance. Each centroid will be located within D -dimensional space and its coordinates will change during training to represent data assignments most appropriately. The parameter N corresponds to sketch *depth* from [17] (number of independent manifold partitionings), while K corresponds to sketch *width* (number of regions produced by each partitioning).

- 2. Embedding projection.** Subsequently, we feed each item modality embedding to a simple linear layer to obtain a projected representation X of dimensionality $N \times K \times D$. This way we bring the input embedding into the D -dimensional space in which the cluster centroids live. After this transformation, input data representation can be represented by its proximity to centroids. The vectors X are batch-normalized.

Distance computation. After bringing input data into the centroid space, we compute the distance between each X and each centroid as $d = (X - C)^2$. This represents a squared distance, but other distance metrics can be used if deemed appropriate. We then sum across D , to obtain squared euclidean distance vectors X_{euclid}

dimensionality $N \times K$. Finally, the obtained representations are normalized with $Y = \text{softmax}(X_{\text{euclid}})$ across the K dimension. The resulting vectors can be thought of as representing soft assignments to K centroids each, over N independent space divisions.

T-EMDE can be implemented in a few lines of code. We attach its pseudocode written in PyTorch convention in Code Listing 1.

```

1 #given depth and width parameters
2 N = 20
3 K = 8
4 inner_dim = 8
5 #input representation size
6 input_dim = 1024
7
8 class Coder(nn.Module):
9     def __init__(self):
10         self.l1 = nn.Linear(input_dim, inner_dim * N
11                               * K)
12         self.bn1 = nn.BatchNorm1d(inner_dim * N * K)
13         self.centroids = nn.Parameter(torch.randn(
14             inner_dim * N * K))
15         self.temp = nn.Parameter(torch.ones(1,))
16
17     #encode individual tokens/image segments
18     def forward(self, x):
19         x = self.l1(x)
20         x = self.bn1(x)
21
22         dists = (x-self.centroids)**2
23         dists = dists.view(-1, N * K, inner_dim).sum(
24             -1).view(-1, N, K)
25         soft_assignments = F.softmax(-dists * self.
26             temp, -1)
27         soft_assignments = soft_assignments.view(-1,
28             N * K)
29         return soft_assignments
30
31 class T_EMDE(nn.Module):
32     def __init__(self):
33         self.coder = Coder()
34
35     #encode a whole text/image
36     def forward(token_embeddings):
37         encoded = self.coder(token_embeddings)
38         summed = torch.sum(encoded, 0)
39         normalized = l2norm(summed.view(-1, N, K),
40             dim=-1).view(-1, K * N)
41         return normalized

```

Code Listing 1: T-EMDE code

It can be seen that T-EMDE exploits the feature space of various modalities, yet at the same time the output vector (the sketch) will represent solely the distances to centroids, losing all modality-specific characteristics. Comparison of two sketches coming from two T-EMDE coders for various modalities (e.g. text and image) will consist in defining the relationships between two sets of centroids.

3.3 SAF and SGR

SAF (Similarity Attention Filtration) and SGR (Similarity Graph Reasoning) are two recent state-of-the art models proposed by [15]. Like most recent cross-modal models, they are complex architectures composed of multiple submodules. They form the backbone of our proposed solution. Below we describe the composing modules

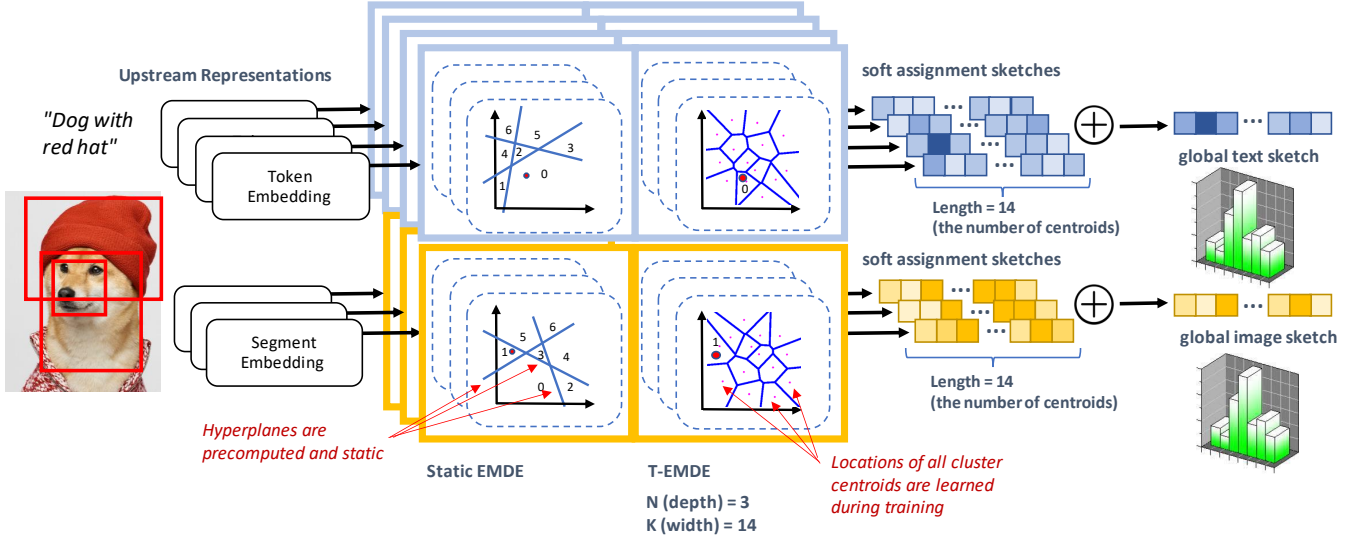


Figure 2: T-EMDE module, with comparison to the static EMDE.

of each solution (some are shared between models). An overview of SAF and SGR architectures is given in Figure 1.

Image Representation. Both models represent images as extracted segment embeddings. Such visual features are computed following [1] to extract K region-level visual features, with the Faster R-CNN [39] model pretrained on Visual Genomes [29]. Only segment embeddings are considered, without recognizing additional features such as segment frame locations or captions. Each segment is projected through a fully-connected layer to transform it to a desired size.

Text Representation. Captions are tokenized with the `nltk` package [35] and each token is represented by a randomly initialized embedding. The embeddings are fed to a bi-directional recurrent GRU network [10] and token representations are obtained by averaging the hidden states from the forward and backward GRU pass.

Global Similarity Module. Global representations are computed for text and image separately with self-attention modules. First, all representations are run through separate sequences of multiple linear layers alternating with batch normalization, to form *local L* and *global G* variants of each modality representations. *Global* representation is obtained by averaging per-segment or per-token representations, while *local* representation consists of token/segment-level vectors. Then, self-attention is computed with a dot product over the two inputs, with *G* repeated to match the number of segments/tokens within *L*:

$$attn_weights = softmax(L \times repeat(G, len(L)))$$

$$new_G = \sum_{j=1}^{n_columns} (attn_weights \cdot L)_{ij}$$

After additional L2-normalization, *new_G* is the final per-modality global representation. Global similarity vector is computed by subtracting the global caption representation from the global image representation.

The Global Similarity Module is one of the computationally heavy parts of the architecture, especially that it needs to be computed two times - always both for text and image. It is replaced with T-EMDE in our solution.

Local Similarity Module. Local Similarity Module also computes attention, but in contrast to Global Similarity Module it is done between the textual and image representations. It uses the cross-modal attention formula from [31] and obtains a summary textual-visual representation.

Similarity Graph Module. This module uses a Graph Neural Network architecture from [30] to model the strength of connection between tokens and image parts. Token/segment local representations together with the global representation computed by the Global Similarity Module are treated as graph nodes within a fully-connected graph. Edges are computed by weighted multiplication of input and output node representations, with each node representation multiplied by trainable matrices W_{in} and W_{out} . Similarity reasoning is performed by summing the edge representations of each node p , multiplied by the representations of neighbors of p , and running them through an extra layer with multiplication against a trainable matrix W_r with a nonlinearity. The global representation nodes are finally fed to a linear layer to return the text-image similarity score.

Similarity Attention Filtration. Similarity Attention Filtration is designed to suppress tokens or segments which have a small influence on the final similarity (such as the function words "a", "be", etc.). It ingests vector similarity representations from previous modules (e.g. Global Similarity and Local Similarity) and runs them through additional linear layers, applying weights assessing

the validity of each similarity alignment. A final linear layer ingesting weighted similarity representations returns the text-image similarity score.

As shown in Figure 1, SAF is composed of two Global Similarity Modules (each per modality), a Local Similarity Module, and the Attention Filtration which computes the final similarity scores. SGR also has two Global Similarity Modules and a Local Similarity Module, followed by Similarity Graph Module.

3.3.1 T-EMDE in SAF/SGR. T-EMDE can be easily introduced in place of the Global Similarity modules (or in fact any other formulation of self-attention). Thanks to the application of two very different neural architectures in SAF and SGR (a graph neural network and an attention filter), the versatility of application of T-EMDE to various architectures can be tested.

The module is applied in the same way to both SAF and SGR, replacing the Global Similarity modules for both image and text. In total, two T-EMDE modules are created, separately for image and text. The segment/token representations fed by the Image Representation and Token Representation modules are fed as input to respective T-EMDE modules. Individual cluster assignments of each token/segment are then retrieved. For each image and caption, the appropriate token/segment soft assignment vectors are summed, exploiting the additivity property of EMDE and Count-Min Sketch [17]. In EMDE, summation is done on item sketches which belong to one shopping basket/user in order to get a global basket/user representation. Similarly in cross-modal retrieval, summation can be thought of as aggregating multiple partwise histograms to get an overview profile of text/image - its global representation. The summation allows for keeping the global representation size constant irrespective of how many composing parts (tokens/segments) need to be aggregated. This mechanism allows us to handle the problem of variable sequence length and escape the necessity of comparing each item to all others which results in quadratic complexity of self-attention.

In contrast to Global Similarity module, the global representations are not subtracted, as corresponding centroids can get assigned to different places in the output sketches. Instead, we concatenate the text and image sketches (this can be done because their size is kept constant at all times) and map them to a smaller size with a linear layer, followed by ReLU activation.

4 EXPERIMENTS

4.1 Datasets

Our evaluation is aligned with [15] for fair comparison, we reuse their evaluation code¹ for full credibility and evaluate on the same datasets. Thus, we use two popular cross-modal datasets: MSCOCO [34] and Flickr30K [58] datasets. The MSCOCO dataset is a large-scale object detection, segmentation, and captioning dataset. It contains 123,287 photos, mainly from daily life scenes. Each image is annotated with 5 captions produced by crowdworkers from Amazon Mechanical Turk. We use a popular cross-modal retrieval split (the ‘‘Karpathy’’ split) which assigns 113,287 images for training, 5,000 images with 25,000 matching captions for validation and 5,000

Table 1: Performance results on the MSCOCO 5K dataset (averaged over 5 runs).

Model	MSCOCO 5K dataset					
	Text Retrieval			Image Retrieval		
	R@1	R@10	MRR	R@1	R@10	MRR
SGM [50]	50.0	87.9	-	35.3	76.5	-
SCAN [31]	50.4	90.0	-	38.6	80.4	-
CAAN [60]	52.5	90.9	-	41.2	82.9	-
VSRN [32]	53.0	89.4	-	40.5	81.1	-
IMRAM [6]	53.7	91.0	-	39.7	79.8	-
SAF noglobal	53.7	90.4	0.663	39.8	80.0	0.532
SAF reported	53.3	90.1	-	39.8	80.2	-
SAF reproduced	55.6	90.7	0.677	40.3	80.3	0.536
T-EMDE	56.7	90.7	0.682	40.3	80.4	0.537
SGR noglobal	54.2	90.3	0.668	39.3	79.3	0.525
SGR reported	56.9	90.5	-	40.2	79.8	-
SGR reproduced	55.7	90.3	0.677	39.8	79.9	0.531
T-EMDE	57.0	91.0	0.685	40.0	80.1	0.533
SGRAF reported	58.8	91.6	-	41.6	81.5	-
SGRAF reproduced	57.9	91.6	0.697	41.8	81.5	0.550
T-EMDE	59.1	91.8	0.703	41.8	81.7	0.551

images with 25,000 matching captions for testing. We use two evaluation protocols:

- MSCOCO 1K - the results are computed by averaging over 5 folds, each of 1000 test images.
- MSCOCO 5K - the results are computed on the full set of 5000 images.

The Flickr30K dataset contains 31,783 images with 5 corresponding captions each. Generally, the Flickr30k captions are much longer and are in many cases more detailed than in MSCOCO. [21]. Following the split in [20], we use 1,000 images for validation, 1,000 images for testing and the rest for training.

4.2 Performance Metrics

As our main performance measure we adapt the Recall@k (R@k) metric applied in [15]. Recall@k can be understood as the proportion of relevant items found in the top-k list of retrieved items. Since the performance of recent cross-modal retrieval models seems to be saturating and the results are often very similar, we also employ an additional performance measure: the mean reciprocal rank (MRR), a popular metric in information retrieval. MRR is the average of the reciprocals of the ranks of the relevant items from the whole query set Q :

$$MRR = \frac{1}{|Q|} \sum_{i=1}^{|Q|} \frac{1}{rank_i}.$$

We compute MRR on T-EMDE, SAF and SGR in order to differentiate their performance results better.

4.3 Training configuration

For the MSCOCO dataset we set $N = 20$ and $K = 8$, and for the Flickr30K - $N = 16$ and $K = 8$, selected experimentally. The inner

¹<https://github.com/Paranioar/SGRAF>

Table 2: Performance results on Flickr30K and MSCOCO 1K datasets (averaged over 5 runs).

Model	Flickr30K dataset								MSCOCO 1K dataset							
	Text Retrieval				Image Retrieval				Text Retrieval				Image Retrieval			
	R@1	R@5	R@10	MRR	R@1	R@5	R@10	MRR	R@1	R@5	R@10	MRR	R@1	R@5	R@10	MRR
CAAN [60]	70.1	91.6	97.2	-	52.8	79.0	87.9	-	75.5	95.4	98.5	-	61.3	89.7	95.2	-
DP-RNN [8]	70.2	91.6	95.8	-	55.5	81.3	88.2	-	75.3	95.8	98.6	-	62.5	89.7	95.1	-
PFAN [51]	70.0	91.8	95.0	-	50.4	78.7	86.1	-	76.5	96.3	99.0	-	61.6	89.6	95.2	-
VSRN [32]	71.3	90.6	96.0	-	54.7	81.8	88.2	-	76.2	94.8	98.2	-	62.8	89.7	95.1	-
IMRAM [6]	74.1	93.0	96.6	-	53.9	79.4	87.2	-	76.7	95.6	98.5	-	61.7	89.1	95.0	-
SAF no global	71.1	91.6	96.3	0.803	54.1	80.7	87.3	0.660	76.2	95.5	98.1	0.845	61.5	89.3	95.1	0.736
SAF reported	73.7	93.3	96.3	-	56.1	81.5	88.0	-	76.1	95.4	98.3	-	61.8	89.4	95.3	-
SAF reproduced	74.9	93.9	97.1	0.833	56.3	81.8	88.0	0.676	77.2	95.7	98.5	0.853	62.1	89.7	95.4	0.741
T-EMDE	75.2	94.2	97.1	0.829	57.1	82.2	88.3	0.682	78.3	95.7	98.5	0.858	62.3	89.7	95.2	0.745
SGR no global	52.8	83.7	92.8	0.664	49.6	77.3	85.1	0.618	76.6	95.8	98.4	0.848	60.9	89.0	95.1	0.731
SGR reported	75.2	93.3	96.6	-	56.2	81.0	86.5	-	78.0	95.8	98.2	-	61.4	89.3	95.4	-
SGR reproduced	76.3	93.2	96.9	0.835	55.2	80.7	88.0	0.666	76.9	95.5	98.5	0.849	61.5	89.4	95.4	0.737
T-EMDE	77.5	93.1	97.2	0.845	56.9	82.0	87.5	0.679	77.1	95.9	98.5	0.852	61.6	89.5	95.1	0.737
SGRAF reported	78.4	94.6	97.5	-	58.2	83.0	89.1	-	79.2	96.2	98.5	-	63.2	90.7	96.1	-
SGRAF reproduced	77.5	94.4	97.0	0.849	58.4	83.2	89.0	0.693	78.9	96.2	98.9	0.864	63.6	90.4	95.8	0.752
T-EMDE	78.8	94.4	97.5	0.858	59.6	83.6	89.2	0.702	79.6	96.3	98.7	0.868	63.5	90.4	95.6	0.752

dimension of the centroid space D is always set to 8 and the centroid distance metric is euclidean distance. All other parameters are as in [15]. T-EMDE/SAF and T-EMDE/SGR are trained separately, and T-EMDE/SGRAF results are computed as average of similarities returned by SAF and SGR (as is done in [15]).

4.4 Results

We present results on Flickr30k and MSCOCO 1K in Table 2 and MSCOCO 5K in Table 1.

We have retrained the original SAF and SGR models, as the original repository uses relatively old library versions - Python v. 2.7, Pytorch v. 0.4.1, and NumPy v. 1.12.1. We have observed mostly higher results after bumping library versions to Python v. 3.6, Pytorch v. 1.7.1, NumPy v. 1.19.5. The original SAF/SGR results from [15] are denoted as SAF/SGR reported while our updated results are SAF/SGR reproduced. Additionally, we also report configurations without the Global Similarity Module as a baseline - SAF/SGR no global. All other competitors are recent top-performing models described in the Related Work Section. We only consider competitors which do not use external data, such as image segment location or segment caption, so that all models use exactly the same sources of information.

We can observe that T-EMDE brings significant improvements in most metrics, especially the R@1 metric (up to 1.7 pp.), in many cases establishing new state-of-the-art results, which leads us to think that it facilitates text/image matching while providing very fine-grained representations. The performance gains can be especially important in practical scenarios, as the R@1 metric denotes the top retrieved items which appear at the start of user recommendation list and determine the first user experience.

The cases where T-EMDE gives non-SOTA results are usually at larger k in Recall@ k (which consider items from lower recommended ranks), and the performance difference to the top-performing

Table 3: Training and inference times of various configurations (averaged over 5 runs).

Model	Flickr 30K		COCO 1K		COCO 5K
	Infer	Train	Infer	Train	Infer
SAF	69.68 s	13h 35m	68.1 s	24h 54m	1725.8 s
T-EMDE	59.68 s	10h 23m	58.1 s	16h 45m	1457.6 s
SGR	83.6 s	17h 35m	84.0 s	48h 52m	2075.0 s
T-EMDE	75.4 s	14h 01m	74.9 s	41h 22m	1830.2 s
SGRAF	161.4 s	-	768.6 s	-	4064.3 s
T-EMDE	135.5 s	-	695.6 s	-	3342.2 s

Table 4: Performance of T-EMDE/SAF on Flickr30K with varying N/K configurations.

N/K	R@1			R@10			MRR		
	8	16	20	8	16	20	8	16	20
20	73.4	73.5	71.4	97.1	95.6	95.2	0.824	0.820	0.805
16	75.3	74.1	73.5	97.1	96.5	96.9	0.829	0.823	0.823
8	74.0	74.3	74.7	97.1	96.4	96.7	0.826	0.820	0.825

model is usually small, from 0.1 to 0.3 pp. In particular, the non-SOTA results appear in T-EMDE/SGRAF MSCOCO 1K Image Retrieval. However, one needs to remember that the MSCOCO 1K evaluation protocol is the approximate version as it averages data chunks and ranking lists are computed on a smaller pool of candidates (a much easier task, hence the marked difference of scores between MSCOCO 1K and MSCOCO 5K which is seen in all models). On the full evaluation protocol - MSCOCO 5K - the T-EMDE models show considerable advantages in scores.

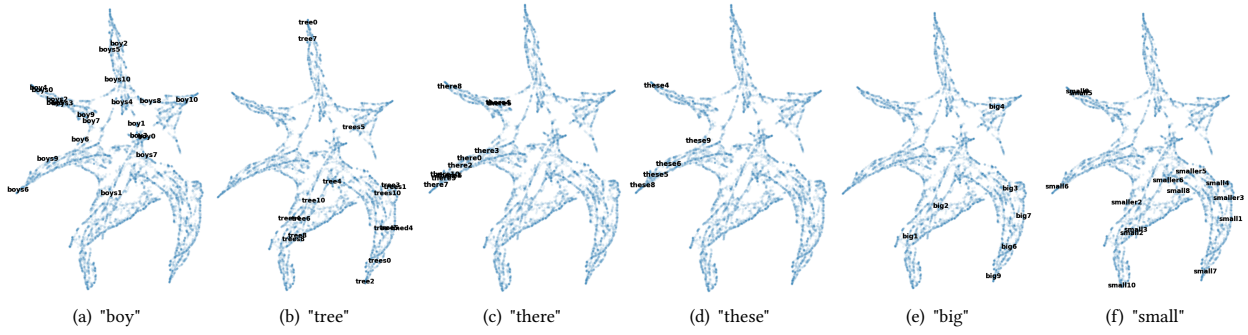


Figure 3: Visualization of particular token locations on a space with 8 centroids mapped to 2D space with U-Map.

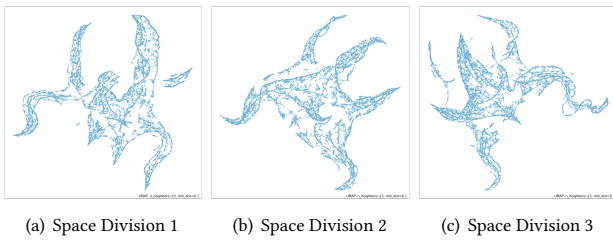


Figure 4: Visualization of token sketches coming from 3 independent space divisions from a single T-EMDE coder, mapped to 2D with U-Map. Each space division features 8 centroids which are discernible in the pictures.

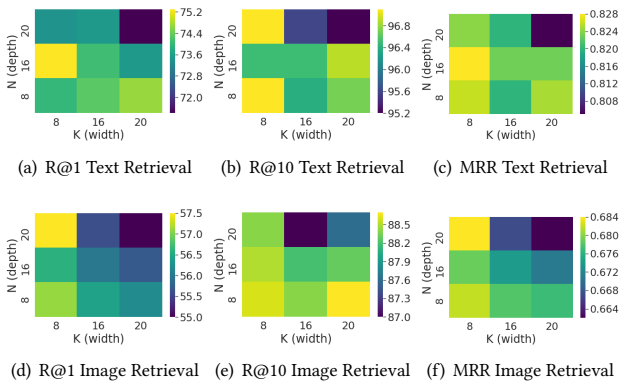


Figure 5: Performance scores on various N/K configurations on Flickr30K dataset.

5 ANALYSIS

5.1 Training and Inference Time

As shown in Table 3, T-EMDE makes both SAF and SGR faster by 15%-20% in every tested scenario in terms of inference time. This difference stems from reducing the quadratic complexity of the global similarity computed with self-attention to linear complexity

of the trainable coder. Such performance difference can be significant in database retrieval scenarios, where low latency is of key importance. Likewise, training times are significantly reduced by a similar proportion as in the case of inference times. Note that the training speed difference does not stem from early stopping, as all benchmarked models were required to complete a defined number of epochs (20 epochs for MSCOCO, 30 epochs for Flickr30K SAF, 40 epochs for Flickr30K SGR).

Benchmarking was performed on a machine with 128 GB RAM, 14 core (28 HT threads) Intel Core i9-9940X 3.30GHz CPUs and GeForce RTX 2080 Ti 11GB GPU.

5.2 Optimal N/K Configuration

In Figure 5 and Table 4 we present $R@1$, $R@10$, and MRR performance scores for various N/K parameter configurations of the T-EMDE/SAF model on the Flickr30K dataset. It can be observed that the T-EMDE sketch size can be indeed small, on the scale of $N \in \{8, 16, 20\}$ and $K = 8$. This is consistent with observations from [17]: too large K results in the loss of the information prior (too many centroids are created and even related items are assigned to different centroids). On the other hand, N can often be large as its function is to introduce an ensembling effect. Independent space partitionings can thus be thought of as individual ensemble models.

Overall, the resulting output sketch dimensionality can be dropped to $N = 8$ and $K = 8$, which produces a particularly small vector of size $8 * 8 = 64$, which is beneficial for model latency. At the same time, the performance loss from a very small coder can be considered low especially in practical scenarios (see Table 4), which allows for further compression of the T-EMDE models.

5.3 Qualitative Analysis

Figure 4 shows 2D U-Map projections of token sketches obtained from T-EMDE, coming from individual space partitionings. The evaluated T-EMDE coder contained 8 centroids, whose locations are discernible in the pictures. Particularly visible are boundary lines composed of individual tokens, akin to Voronoi cell boundaries. This suggests that many tokens are purposefully placed at equal distances to multiple centroids.

In Figure 3 we display the results of a 2D projection of a single 8-centroid space partitioning, but with annotated locations of particular tokens. It can be seen that various token classes occupy

particular regions in space. For example, the words denoting sizes - *big* and *small* tend to group rather at the right bottom "legs" of the visualization. An interesting case are the function words (exemplified with *there* and *these*) which are common in captions but bring in little semantic value. Such words are clearly grouped in a single cluster, which seems purposeful so that they can be ignored by the rest of the network.

6 CONCLUSIONS

In this paper we have presented T-EMDE - a highly efficient module for computing global representations of text and image in multi-modal retrieval scenarios. By replacing a self-attentive module in recent high-performing architectures, we are able to reach new state-of-the-art results on MSCOCO and Flickr30k datasets, with especially significant gains in the Recall@1 metric. At the same time, we reduce the model latency by up to 20%. We propose T-EMDE as a step in the direction of replacing computationally expensive self-attention with more efficient approaches.

REFERENCES

- [1] Peter Anderson, Xiaodong He, Chris Buehler, Damien Teney, Mark Johnson, Stephen Gould, and Lei Zhang. 2018. Bottom-Up and Top-Down Attention for Image Captioning and Visual Question Answering. In *2018 IEEE Conference on Computer Vision and Pattern Recognition, CVPR 2018, Salt Lake City, UT, USA, June 18-22, 2018*. IEEE Computer Society, 6077–6086. <https://doi.org/10.1109/CVPR.2018.00636>
- [2] Dzmitry Bahdanau, Kyung Hyun Cho, and Yoshua Bengio. 2015. Neural machine translation by jointly learning to align and translate. In *3rd International Conference on Learning Representations, ICLR 2015 - Conference Track Proceedings*. International Conference on Learning Representations, ICLR. arXiv:1409.0473 <https://arxiv.org/abs/1409.0473v7>
- [3] Jiyang Bai, Yuxiang Ren, and J. Zhang. 2020. Ripple Walk Training: A Subgraph-based training framework for Large and Deep Graph Neural Network. *ArXiv abs/2002.07206* (2020).
- [4] Irwan Bello. [n.d.]. LambdaNetworks: Modeling long-range Interactions without Attention. In *International Conference on Learning Representations (ICLR) 2021*.
- [5] Iz Beltagy, Matthew E. Peters, and Arman Cohan. 2020. *Longformer: The Long-Document Transformer*. Technical Report. arXiv:2004.05150 <https://github.com/allenai/longformer>
- [6] Hui Chen, Guiguang Ding, Xudong Liu, Zijia Lin, Ji Liu, and Jungong Han. 2020. IMRAM: Iterative Matching with Recurrent Attention Memory for Cross-Modal Image-Text Retrieval. *Proceedings of the IEEE Computer Society Conference on Computer Vision and Pattern Recognition (mar 2020)*, 12652–12660. <https://doi.org/10.1109/CVPR42600.2020.01267> arXiv:2003.03772
- [7] Jianfei Chen, Jun Zhu, and Le Song. [n.d.]. Stochastic Training of Graph Convolutional Networks with Variance Reduction. In *Proceedings of the 35th International Conference on Machine Learning*.
- [8] Tianlang Chen and Jiebo Luo. 2020. Expressing objects just like words: Recurrent visual embedding for image-text matching. *arXiv* (feb 2020). <https://doi.org/10.1609/aaai.v34i07.6631> arXiv:2002.08510
- [9] Rewon Child, Scott Gray, Alec Radford, and Ilya Sutskever. 2019. *Generating long sequences with sparse transformers*. Technical Report. arXiv:1904.10509 <https://openai.com/blog/sparse-transformer>
- [10] Kyunghyun Cho, Bart van Merriënboer, Dzmitry Bahdanau, and Yoshua Bengio. 2014. On the Properties of Neural Machine Translation: Encoder–Decoder Approaches. In *Proceedings of SSST-8, Eighth Workshop on Syntax, Semantics and Structure in Statistical Translation*. Association for Computational Linguistics, Doha, Qatar, 103–111. <https://doi.org/10.3115/v1/W14-4012>
- [11] Krzysztof Choromanski, Valerii Likhoshesterov, David Dohan, Xingyou Song, Andreea Gane, Tamas Sarlos, Peter Hawkins, Jared Davis, Afroz Mohiuddin, Lukasz Kaiser, David Belanger, Lucy Colwell, and Adrian Weller. 2020. *Rethinking attention with performers*. Technical Report. arXiv:2009.14794
- [12] Junyoung Chung, Çağlar Gulcehre, KyungHyun Cho, and Yoshua Bengio. 2014. *Empirical Evaluation of Gated Recurrent Neural Networks on Sequence Modeling*. Technical Report. arXiv:1412.3555 <http://arxiv.org/abs/1412.3555>
- [13] Zihang Dai, Zhilin Yang, Yiming Yang, Jaime Carbonell, Quoc V. Le, and Ruslan Salakhutdinov. 2020. *Transformer-XL: Attentive language models beyond a fixed-length context*. Technical Report. 2978–2988 pages. <https://doi.org/10.18653/v1/p19-1285> arXiv:1901.02860
- [14] Priya Deshpande, Alexander Rasin, Eli Brown, Jacob Furst, Daniela Raicu, Steven Montner, and Samuel Armato III. 2017. An Integrated Database and Smart Search Tool for Medical Knowledge Extraction from Radiology Teaching Files. In *Proceedings of The First Workshop Medical Informatics and Healthcare held with the 23rd SIGKDD Conference on Knowledge Discovery and Data Mining (Proceedings of Machine Learning Research, Vol. 69)*, Samah Fodeh and Daniela Stan Raicu (Eds.). PMLR, 10–18. <http://proceedings.mlr.press/v69/deshpande17a.html>
- [15] Haiwen Diao, Ying Zhang, Lin Ma, and Huchuan Lu. [n.d.]. Similarity Reasoning and Filtration for Image-Text Matching. In *AAAI 2021*.
- [16] Alexey Dosovitskiy, Lucas Beyer, Alexander Kolesnikov, Dirk Weissenborn, Xi-aohua Zhai, Thomas Unterthiner, Mostafa Dehghani, Matthias Minderer, Georg Heigold, Sylvain Gelly, Jakob Uszkoreit, and Neil Houlsby. 2020. An Image is Worth 16x16 Words: Transformers for Image Recognition at Scale. (oct 2020). arXiv:2010.11929 <http://arxiv.org/abs/2010.11929>
- [17] Jacek Dąbrowski, Barbara Rychalska, Michał Daniluk, Dominika Basaj, Piotr Babel, Andrzej Michałowski, and Adam Jakubowski. 2021. An efficient manifold density estimator for all recommendation systems. <https://arxiv.org/abs/2006.01894>
- [18] Benjamin Elizalde, Shuayb Zarar, and Bhiksha Raj. 2019. Cross Modal Audio Search and Retrieval with Joint Embeddings Based on Text and Audio. In *ICASSP 2019 - 2019 IEEE International Conference on Acoustics, Speech and Signal Processing (ICASSP)*. 4095–4099. <https://doi.org/10.1109/ICASSP.2019.8682632>
- [19] Fartash Faghri, David J. Fleet, Jamie Ryan Kiros, and Sanja Fidler. 2017. VSE++: Improving visual-semantic embeddings with hard negatives. *arXiv* (jul 2017). arXiv:1707.05612 <http://arxiv.org/abs/1707.05612>
- [20] Andrea Frome, Greg S Corrado, Jon Shlens, Samy Bengio, Jeff Dean, Marc’Aurelio Ranzato, and Tomas Mikolov. 2013. DeViSE: A Deep Visual-Semantic Embedding Model. In *Advances in Neural Information Processing Systems*, C. J. C. Burges, L. Bottou, M. Welling, Z. Ghahramani, and K. Q. Weinberger (Eds.), Vol. 26. Curran Associates, Inc. <https://proceedings.neurips.cc/paper/2013/file/7cce53cf90577442771720a370c3c723-Paper.pdf>
- [21] Zhibin Guan, Kang Liu, Ma Yan, Xu Qian, and Tongkai Ji. 2018. Sequential Dual Attention: Coarse-to-Fine-Grained Hierarchical Generation for Image Captioning. *Symmetry* 10 (11 2018), 626. <https://doi.org/10.3390/sym10110626>
- [22] MD. Zakir Hossain, Ferdous Sohel, Mohd Fairuz Shiratuddin, and Hamid Laga. 2019. A Comprehensive Survey of Deep Learning for Image Captioning. *ACM Comput. Surv.* 51, 6, Article 118 (Feb. 2019), 36 pages. <https://doi.org/10.1145/3295748>
- [23] Zhibin Hu, Yongsheng Luo, Jiong Lin, Yan Y. Yan, and Jian Chen. 2019. Multi-level visual-semantic alignments with relation-wise dual attention network for image and text matching. In *IJCAI International Joint Conference on Artificial Intelligence*, Vol. 2019-August. International Joint Conferences on Artificial Intelligence, 789–795. <https://doi.org/10.24963/ijcai.2019/111>
- [24] Lun Huang, Wenmin Wang, Jie Chen, and Xiao-Yong Wei. 2019. Attention on Attention for Image Captioning. In *Proceedings of the IEEE/CVF International Conference on Computer Vision (ICCV)*.
- [25] Po-Yao Huang, Xiaojun Chang, Alexander Hauptmann, and Eduard Hovy. 2020. Forward and Backward Multimodal NMT for Improved Monolingual and Multilingual Cross-Modal Retrieval. In *Proceedings of the 2020 International Conference on Multimedia Retrieval (Dublin, Ireland) (ICMR ’20)*. Association for Computing Machinery, New York, NY, USA, 53–62. <https://doi.org/10.1145/3372278.3390674>
- [26] Andrej Karpathy and Li Fei-Fei. 2017. Deep Visual-Semantic Alignments for Generating Image Descriptions. *IEEE Transactions on Pattern Analysis and Machine Intelligence* 39, 4 (dec 2017), 664–676. <https://doi.org/10.1109/TPAMI.2016.2598339> arXiv:1412.2306
- [27] Angelos Katharopoulos, Apoorv Vyas, Nikolaos Pappas, and François Fleuret. 2020. Transformers are RNNs: Fast Autoregressive Transformers with Linear Attention. *arXiv* (jun 2020). arXiv:2006.16236 <http://arxiv.org/abs/2006.16236>
- [28] Nikita Kitaev, Łukasz Kaiser, and Anselm Levskaya. 2020. *Reformer: the Efficient Transformer*. Technical Report. arXiv:2001.04451 <https://hackingsemantics.xyz/2019/leaderboards/>
- [29] Ranjay Krishna, Yuke Zhu, Oliver Groth, Justin Johnson, Kenji Hata, Joshua Kravitz, Stephanie Chen, Yannis Kalantidis, Li-Jia Li, David A. Shamma, Michael S. Bernstein, and Li Fei-Fei. 2017. Visual Genome: Connecting Language and Vision Using Crowdsourced Dense Image Annotations. *Int. J. Comput. Vis.* 123, 1 (2017), 32–73. <https://doi.org/10.1007/s11263-016-0981-7>
- [30] Zhanghui Kuang, Yiming Gao, Guanbin Li, Ping Luo, Yimin Chen, Liang Lin, and Wayne Zhang. 2019. Fashion Retrieval via Graph Reasoning Networks on a Similarity Pyramid. In *2019 IEEE/CVF International Conference on Computer Vision, ICCV 2019, Seoul, Korea (South), October 27 - November 2, 2019*. IEEE, 3066–3075. <https://doi.org/10.1109/ICCV.2019.00316>
- [31] Kuang Huei Lee, Xi Chen, Gang Hua, Houdong Hu, and Xiaodong He. 2018. Stacked Cross Attention for Image-Text Matching. *Lecture Notes in Computer Science (including subseries Lecture Notes in Artificial Intelligence and Lecture Notes in Bioinformatics)* 11208 LNCS (mar 2018), 212–228. https://doi.org/10.1007/978-3-030-01225-0_13 arXiv:1803.08024

- [32] Kunpeng Li, Yulun Zhang, Kai Li, Yuanyuan Li, and Yun Fu. 2019. Visual semantic reasoning for image-text matching. *Proceedings of the IEEE International Conference on Computer Vision 2019-October* (sep 2019), 4653–4661. <https://doi.org/10.1109/ICCV.2019.00475> arXiv:1909.02701
- [33] Shuang Li, Tong Xiao, Hongsheng Li, Bolei Zhou, Dayu Yue, and Xiaogang Wang. 2017. Person Search With Natural Language Description. In *Proceedings of the IEEE Conference on Computer Vision and Pattern Recognition (CVPR)*.
- [34] Tsung-Yi Lin, Michael Maire, Serge J. Belongie, James Hays, Pietro Perona, Deva Ramanan, Piotr Dollár, and C. Lawrence Zitnick. 2014. Microsoft COCO: Common Objects in Context. In *Computer Vision - ECCV 2014 - 13th European Conference, Zurich, Switzerland, September 6-12, 2014, Proceedings, Part V (Lecture Notes in Computer Science, Vol. 8693)*, David J. Fleet, Tomás Pajdla, Bernt Schiele, and Tinne Tuytelaars (Eds.). Springer, 740–755. https://doi.org/10.1007/978-3-319-10602-1_48
- [35] Edward Loper and Steven Bird. 2002. NLTK: The Natural Language Toolkit. In *In Proceedings of the ACL Workshop on Effective Tools and Methodologies for Teaching Natural Language Processing and Computational Linguistics*. Philadelphia: Association for Computational Linguistics.
- [36] Tetsuro Nishihara, Akihiro Tamura, Takashi Ninomiya, Yutaro Omote, and Hideki Nakayama. 2020. Supervised Visual Attention for Multimodal Neural Machine Translation. In *Proceedings of the 28th International Conference on Computational Linguistics*. International Committee on Computational Linguistics, Barcelona, Spain (Online), 4304–4314. <https://doi.org/10.18653/v1/2020.coling-main.380>
- [37] Jiezhong Qiu, Hao Ma, Omer Levy, Scott Wen Tau Yih, Sinong Wang, and Jie Tang. 2019. Blockwise self-attention for long document understanding. *arXiv* (nov 2019). <https://doi.org/10.18653/v1/2020.findings-emnlp.232> arXiv:1911.02972
- [38] Colin Raffel, Noam Shazeer, Adam Roberts, Katherine Lee, Sharan Narang, Michael Matena, Yanqi Zhou, Wei Li Peter, and J. Liu. 2019. *Exploring the limits of transfer learning with a unified text-to-text transformer*. Technical Report. 1–67 pages. arXiv:1910.10683 <http://jmlr.org/papers/v21/20-074.html>.
- [39] Shaoqing Ren, Kaiming He, Ross Girshick, and Jian Sun. 2015. Faster R-CNN: Towards Real-Time Object Detection with Region Proposal Networks. In *Advances in Neural Information Processing Systems*, C. Cortes, N. Lawrence, D. Lee, M. Sugiyama, and R. Garnett (Eds.), Vol. 28. Curran Associates, Inc. <https://proceedings.neurips.cc/paper/2015/file/14bfa6bb14875e45bba028a21ed38046-Paper.pdf>
- [40] Aurko Roy, Mohammad Saffar, Ashish Vaswani, and David Grangier. 2020. *Efficient content-based sparse attention with routing transformers*. Technical Report. https://doi.org/10.1162/tacl_a_00353 arXiv:2003.05997
- [41] Yale Song and Mohammad Soleymani. 2019. Polysemous visual-semantic embedding for cross-modal retrieval. *Proceedings of the IEEE Computer Society Conference on Computer Vision and Pattern Recognition 2019-June* (jun 2019), 1979–1988. <https://doi.org/10.1109/CVPR.2019.00208> arXiv:1906.04402
- [42] Weijie Su, Xizhou Zhu, Yue Cao, Bin Li, Lewei Lu, Furu Wei, and Jifeng Dai. 2019. *VL-BERT: Pre-training of generic visual-linguistic representations*. Technical Report. arXiv:1908.08530 <https://github.com/jackroos/VL-BERT>.
- [43] Hao Tan and Mohit Bansal. 2020. *LXMert: Learning cross-modality encoder representations from transformers*. Technical Report. 5100–5111 pages. <https://doi.org/10.18653/v1/d19-1514> arXiv:1908.07490
- [44] Yi Tay, Dara Bahri, Liu Yang, Donald Metzler, and Da Cheng Juan. 2020. *Sparse sinkhorn attention*. Technical Report. arXiv:2002.11296
- [45] Yi Tay, Da Cheng Juan, Dara Bahri, Zhe Zhao, Donald Metzler, and Che Zheng. 2020. *SYNTHESIZER: Rethinking Self-Attention in Transformer Models*. Technical Report. arXiv:2005.00743
- [46] Ashish Vaswani, Noam Shazeer, Niki Parmar, Jakob Uszkoreit, Llion Jones, Aidan N. Gomez, Łukasz Kaiser, and Illia Polosukhin. 2017. Attention is all you need. In *Advances in Neural Information Processing Systems*, Vol. 2017-December. Neural information processing systems foundation, 5999–6009. arXiv:1706.03762 <https://arxiv.org/abs/1706.03762v5>
- [47] Madhusudan Verma. 2021. Beyond Nystromformer—Approximation of self-attention by Spectral Shifting. *arXiv preprint arXiv:2103.05638* (2021).
- [48] Liwei Wang, Yin Li, and Svetlana Lazebnik. 2016. Learning deep structure-preserving image-text embeddings. *Proceedings of the IEEE Computer Society Conference on Computer Vision and Pattern Recognition 2016-December* (nov 2016), 5005–5013. <https://doi.org/10.1109/CVPR.2016.541> arXiv:1511.06078
- [49] Sinong Wang, Belinda Z. Li, Madian Khabsa, Han Fang, and Hao Ma. 2020. Linformer: Self-Attention with Linear Complexity. *arXiv* (jun 2020). arXiv:2006.04768 <http://arxiv.org/abs/2006.04768>
- [50] Sijin Wang, Ruiping Wang, Ziwei Yao, Shiguang Shan, and Xilin Chen. 2020. Cross-modal scene graph matching for relationship-aware image-text retrieval. *Proceedings - 2020 IEEE Winter Conference on Applications of Computer Vision, WACV 2020* (oct 2020), 1497–1506. <https://doi.org/10.1109/WACV45572.2020.9093614> arXiv:1910.05134
- [51] Yaxiong Wang, Hao Yang, Xueming Qian, Lin Ma, Jing Lu, Biao Li, and Xin Fan. 2019. Position focused attention network for image-text matching. *IJCAI International Joint Conference on Artificial Intelligence 2019-August* (jul 2019), 3792–3798. <https://doi.org/10.24963/ijcai.2019/526> arXiv:1907.09748
- [52] Xi Wei, Tianzhu Zhang, Yan Li, Yongdong Zhang, and Feng Wu. 2020. *Multi-modality cross attention network for image and sentence matching*. Technical Report. 10938–10947 pages. <https://doi.org/10.1109/CVPR42600.2020.01095>
- [53] Bichen Wu, Chenfeng Xu, Xiaoliang Dai, Alvin Wan, Peizhao Zhang, Masayoshi Tomizuka, Kurt Keutzer, and Peter Vajda. 2020. Visual Transformers: Token-based Image Representation and Processing for Computer Vision. *arXiv* (jun 2020). arXiv:2006.03677 <http://arxiv.org/abs/2006.03677>
- [54] Lemeng Wu, Xingchao Liu, and Qiang Liu. 2021. Centroid Transformers: Learning to Abstract with Attention. (feb 2021). arXiv:2102.08606 <http://arxiv.org/abs/2102.08606>
- [55] Kelvin Xu, Jimmy Lei Ba, Ryan Kiros, Kyunghyun Cho, Aaron Courville, Ruslan Salakhutdinov, Richard S. Zemel, and Yoshua Bengio. 2015. Show, attend and tell: Neural image caption generation with visual attention. In *32nd International Conference on Machine Learning, ICML 2015*, Vol. 3. International Machine Learning Society (IMLS), 2048–2057. arXiv:1502.03044 <https://arxiv.org/abs/1502.03044v3>
- [56] Ruiqing Xu, Chao Li, Junchi Yan, Cheng Deng, and Xianglong Liu. 2019. Graph Convolutional Network Hashing for Cross-Modal Retrieval. In *Proceedings of the Twenty-Eighth International Joint Conference on Artificial Intelligence, IJCAI 2019, Macao, China, August 10-16, 2019*, Sarit Kraus (Ed.), ijcai.org, 982–988. <https://doi.org/10.24963/ijcai.2019/138>
- [57] Ting Yao, Yingwei Pan, Yehao Li, and Tao Mei. 2018. Exploring Visual Relationship for Image Captioning. In *Proceedings of the European Conference on Computer Vision (ECCV)*.
- [58] Peter Young, Alice Lai, Micah Hodosh, and Julia Hockenmaier. 2014. From image descriptions to visual denotations: New similarity metrics for semantic inference over event descriptions. *Trans. Assoc. Comput. Linguistics* 2 (2014), 67–78. <https://tacl2013.cs.columbia.edu/ojs/index.php/tacl/article/view/229>
- [59] Hanqing Zeng, Hongkuan Zhou, Ajitesh Srivastava, Rajgopal Kannan, and Viktor Prasanna. [n.d.]. Accurate, efficient and scalable training of Graph Neural Networks. *J. Parallel and Distrib. Comput.* ([n.d.]).
- [60] Qi Zhang, Zhen Lei, Zhaoxiang Zhang, and Stan Z Li. [n.d.]. *Context-Aware Attention Network for Image-Text Retrieval*. Technical Report.
- [61] Wentian Zhao, Xinxiao Wu, and Jiebo Luo. 2021. Cross-Domain Image Captioning via Cross-Modal Retrieval and Model Adaptation. *IEEE Transactions on Image Processing* 30 (2021), 1180–1192. <https://doi.org/10.1109/TIP.2020.3042086>
- [62] Zhedong Zheng, Liang Zheng, Michael Garrett, Yi Yang, and Yi Dong Shen. 2017. Dual-path convolutional image-text embeddings with instance loss. *arXiv* (nov 2017). arXiv:1711.05535 <http://arxiv.org/abs/1711.05535>